Aspect of oscillatory along-shelf flow in the vicinity of an isolated submarine canyon

Don L. Boyer, A. N. Srdic, Sergey A. Smirnov, D. B. Haidvogel, Joël Sommeria

Aspects of oscillatory along-shelf flow in the vicinity of an isolated submarine canyon

D.L. Boyer, A.N. Srdic & S.A. Smirnov
Arizona State University, Tempe, AZ, USA

D.B. Haidvogel
Institute of Marine and Coastal Sciences, Rutgers University, New Brunswick, NJ, USA

J. Sommeria
CNRS, LEGI Coriolis, Grenoble, France

ABSTRACT: Selected results are presented from a closely coupled laboratory-numerical model study of the oscillatory flow of a linearly stratified fluid in the vicinity of an isolated submarine canyon. It is shown that the boundary condition applied along the model floor in the numerical experiments is critically important in having the numerical model simulate the laboratory experiments. Furthermore, it is shown that enhanced viscosities, which assure the numerical stability, must be applied with care because they may change the flow fields. A scaling argument is advanced which predicts the strength of the time-mean flow generated by the background current. The sensitivity of the flow field to changes in some of the system parameters is discussed. Finally, some initial results for flows generated in the presence of boundary turbulence are also discussed.

1 INTRODUCTION

In recent communications by three of us, comparisons of the flow fields obtained by a series of laboratory experiments and an associated numerical model were made with the goal of determining the degree to which laboratory experiments could be used in the development of numerical models of coastal currents; see Pérenne et al. 2001 and Boyer et al. 2003, henceforth designated as PHB and BHP, respectively. The motivations for these studies were based on (i) the recognition that current numerical models when applied to the same forcing and boundary conditions can provide enormously different results when strict one to one comparisons are made (see, Haidvogel & Beckmann (1998)); (ii) the difficulty of field programs providing adequate data in space and time to test the models; (iii) the understanding that most of the physics of the coastal oceans can be modeled to some degree in the laboratory; and (iv) the realization that modern data acquisition techniques such as Particle tracking velocimetry (PTV) and particle image velocimetry (PIV) can provide data sets having characteristics similar to those generated by numerical models.

The idealized physical system considered is given schematically in Figure 1. An annular coast (vertical), shelf (horizontal) and continental slope model, incised by a single submarine canyon, is placed in the central portion of a circular test cell; the deep ocean is between the continental slope and the outside wall of the test cell. The test cell is filled with a linearly stratified fluid whilst rotating and the initial background rotation is set at $f/2$, where f is the Coriolis parameter. After the fluid has reached the state of a solid-body rotation, experiments are initiated by modulating harmonically the test cell with an amplitude $\Delta\Omega$ and a period T about the background rotation rate $f/2$.

A dimensional analysis shows that four dynamical (the Rossby, Ro; temporal Rossby, Ro_t; Burger, Bu; and Ekman, E, numbers) and five geometrical parameters characterize the system. Laboratory experiments for laminar flows have been conducted in a 1.8 m diameter test cell at Arizona State University in Tempe, Arizona, while transitional and fully developed turbulent flows employed the 13 m diameter tank of the Laboratoire des Ecoulements Geophysiques et Industriels (LEGI) in Grenoble, France. The Tempe, Arizona, and Grenoble, France, experiments used PTV and PIV, techniques, to obtain the time dependent horizontal velocity fields at selected levels. The numerical model employed was the Spectral Element Ocean Model (SEOM) described in Haidvogel & Beckmann (1999). The SEOM used a parameterized shear stress condition

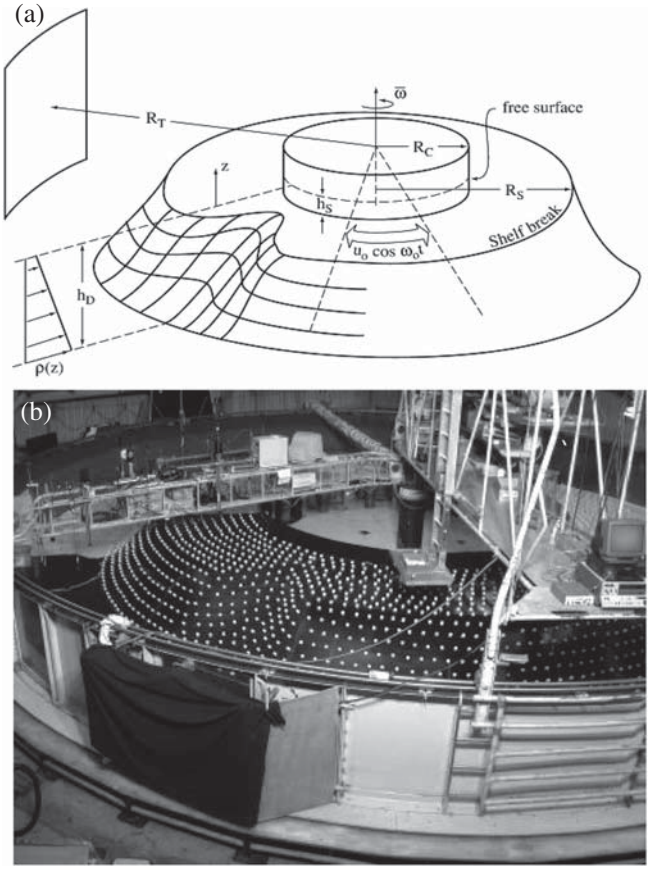

Figure 1. Experimental set-up (a) schematic of the canyon model, (b) rotating tank and the canyon model with roughness elements in Grenoble.

Table 1. Dimensionless parameters.

Parameter	Tempe	Grenoble	Ocean
Rossby number	0.1	0.14	0.14–0.43
Temporal Rossby number	0.25–1.25	0.5	<1
Burger number	2.5–10	1.35	5–18
Ekman number	3.2×10^{-3}	1.2×10^{-4}	4×10^{-7}

for most of the experiments and, to assure numerical stability, employed enhanced horizontal viscosities (i.e., 100 times larger than the kinematic viscosity of the water). Table 1 provides definitions of the various dimensionless parameters as well as their values and/or ranges for experiments in Tempe and Grenoble as well as in the ocean.

This communication will touch briefly three aspects of the overall study. These include (i) the reasons why the numerical simulations in PHB do not fall within the error bars of the physical experiments, (ii) the sensitivity of the time mean flows to the changes in the system parameters, and (iii) a discussion of the preliminary experiments for turbulent flows emphasizing similarities and differences between their laminar counterparts.

2 SELECTED RESULTS

2.1 *Variance between laboratory and numerical models*

The PHB study exhibited substantial differences between the laboratory and numerical models. These model-model differences can be shown to owe to the lack of sufficient resolution of the Ekman layers along the model floor. Even with the Ekman layers adequately resolved, the numerical solutions are not totally satisfactory in that enhanced viscosities must be employed for both the parameterized shear stress and resolved Ekman layer (no-slip) boundary conditions. Presumably, if the resolution of the numerical models could be increased, the SEOM model would presumably give a satisfactory simulation of the flow.

Figures 2a, b, c are illustrations of the velocity fields for (i) the laboratory experiments, (ii) the SEOM model using the shear stress parameterization and (iii) the SEOM model using the no slip condition, respectively. The SEOM model with the stress boundary conditions gives a good simulation qualitatively but on a closer look the quantitative differences are well above the error bars of the laboratory measurements. Additionally the laboratory vorticity and divergence fields are more symmetric about the canyon axis than the numerical model using the shear stress condition. Figures 2c for the SEOM model for which the no-slip condition has been applied, does a better job of simulating the across-axis symmetry of the observations. Furthermore the magnitudes of the maximum vorticity and divergence are correct within the uncertainties of the experiments. The real difficulty is that the numerics required enhanced horizontal viscosities to maintain the numerical stability. This viscosity coupled with the no-slip condition leads to thicker aerodynamic boundary layers along the canyon walls. Such layers, of course, are not found in nature. Presumably, given sufficient resolution, the SEOM model should be able to satisfactorily simulate the laboratory experiment.

2.2 *Sensitivity to parameter variations*

The PHB study focused on a single set of system parameters, which we note as the central case. The question arises as to what degree does the flow field change with variations in the system parameters. Let us first discuss a number of case studies and choose as an observable the time mean or residual flow in the horizontal plane of the shelf break.

Figures 3a, b, c, d depict the velocity and vorticity fields for the laboratory experiments (left) and shear–stress condition SEOM numerical model runs (right)

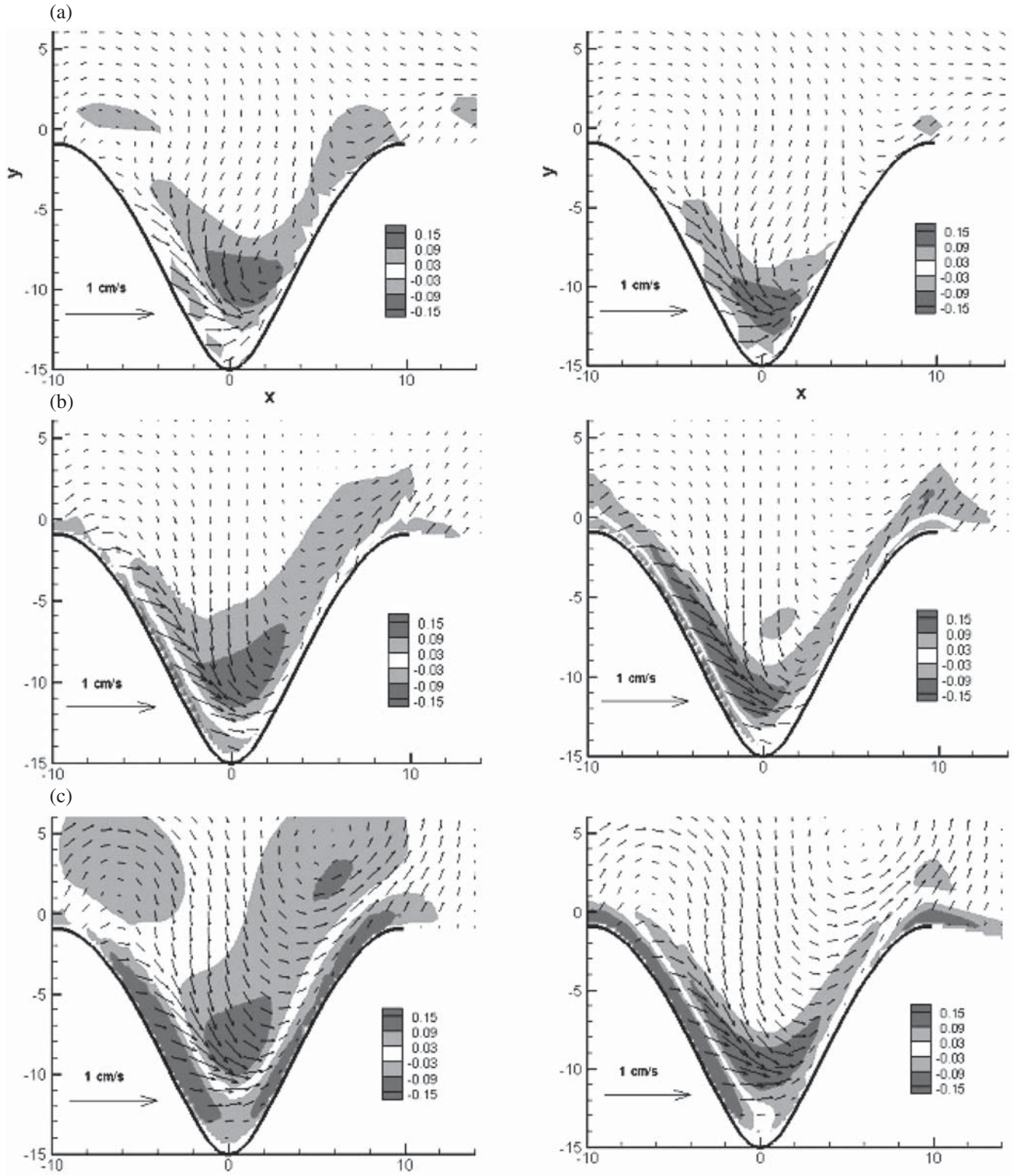

Figure 2. Vorticity (left) and horizontal divergence (right) fields for the central experiment discussed by PHB as obtained from (a) the laboratory, (b) the SEOM model using a parameterized shear–strees condition along the model floor and (c) the SEOM model using a no-slip condition, including a highly resolved Ekman layer, along the model floor. Parameters: $Ro = 0.1$, $Ro_t = 0.52$, $Bu = 10$, $E = 3.2 \times 10^{-3}$.

for the plane of the shelf break for the central case and three other cases to be described below. Figure 3a is for the central case and shows a rather strong region of cyclonic vorticity in the head of the canyon. The only parameter changed in Figure 3b from that of 3a is the Burger number that has been reduced a factor of 4. Thus, Figure 3b can be considered identical to 3a, although having a significantly weaker stratification. This, in turn, leads to a much stronger mean or residual flow; the flow distribution for the turbulent case is

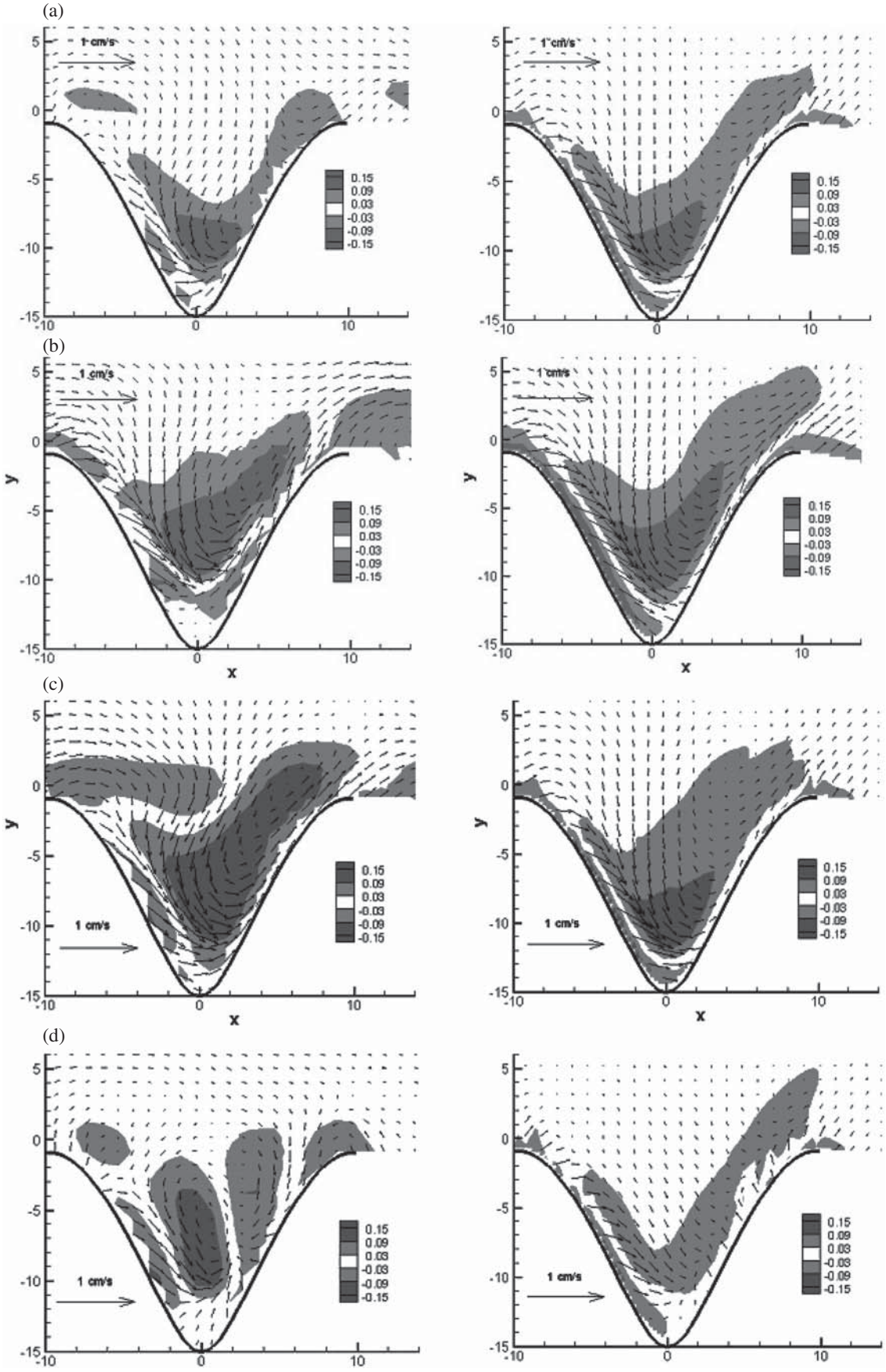

Figure 3. Velocity and vorticity fields for laboratory (left) and SEOM (right) models at the shelf-break level $z/h_D = -0.2$ for (a) $Ro = 0.1$, $Ro_t = 0.52$, $Bu = 10$, $E = 3.2 \times 10^{-3}$; (b) $Ro = 0.1$, $Ro_t = 0.52$, $Bu = 2.5$, $E = 3.2 \times 10^{-3}$; (c) $Ro = 0.1$, $Ro_t = 0.25$, $Bu = 10$, $E = 3.2 \times 10^{-3}$; (d) $Ro = 0.1$, $Ro_t = 1.25$, $Bu = 10$, $E = 3.2 \times 10^{-3}$.

also more uniform in the vertical direction for the less stratified case.

The parameter values for Figure 3c are the same as those for Figure 3a with the exception that $Ro_t = 0.25$ in 3c rather than 0.52 in 3a. This illustration shows that the characteristic speed of the shelf break vorticity is less than that for 3a, in keeping with the scaling argument given below. Figure 3d corresponds to $Ro_t = 1.25$ and gives the vorticity and velocity fields for the superinertial counterpart of 3a, which shows that the cyclonic vorticity at the shelf break level is also stronger for the lower temporal Rossby number case. One notes, that the nature of the multicell mean flow regime for the super-inertial case is not captured by the SEOM model. The reason for this is not apparent at the present moment.

A numerical model comparison for the energetics of increasing *Ro* numbers, other parameters held fixed, was conducted by the SEOM model and showed a strong increase with *Ro*. Furthermore, a laboratory experiment was conducted in the 13.5 m diameter tank of LEGI in which a scaled up version of the model being considered was investigated. This experiment demonstrated that although the Ekman number becomes increasingly small, its effects on the flow dynamics does not become negligible.

BHP advanced a scaling argument for the magnitude of the normalized time mean flow speed based on the system parameters for the magnitude of the normalized time mean flow. The scaling argument used the notion that the vortex tubes with a vertical orientation are stretched in passing from the shelf, across the shelf break and into the canyon. During one oscillation cycle, this stretching leads to a predominantly cyclonic vorticity; the cyclonic vorticity production Z during this period can be shown to scale as

$$Z \sim \frac{h_D}{h_S} \frac{Ro}{Ro_t Bu^{1/2}} u_0 L , \qquad (2.1)$$

where $h_D =$ deep-ocean depth, $h_S =$ the depth at the shelf, $L =$ the length of the continental slope, $u_0 =$ the characteristic velocity at the shelf-break.

This vorticity production per cycle must be dissipated in each cycle. To this end, it is assumed that the dissipation, *D*, takes place on the boundaries of the canyon by Ekman suction; the scaling for Ekman suction can be written as (Pedlosky, 1979)

$$D \sim E^{1/2} \zeta_B W L , \qquad (2.2)$$

where $\zeta_B =$ the basin-scale vorticity, $W =$ the width of the canyon. Equating (2.1) and (2.2), one obtains

$$\frac{\overline{U_1}}{u_0} \sim \frac{Ro}{(h_S / h_D) Ro_t Bu^{1/2} E^{1/2}} = \lambda . \qquad (2.3)$$

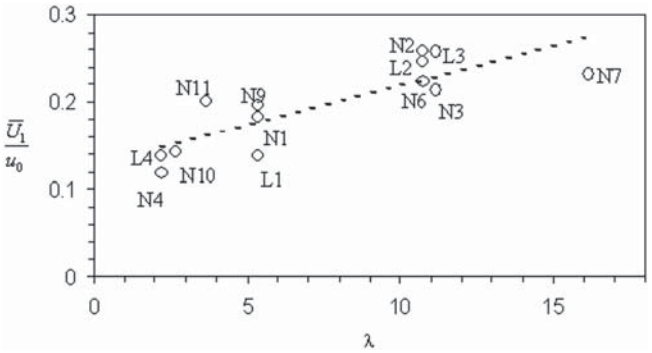

Figure 4. Characteristic speed of the normalized time-mean flow at the shelf break level as obtained from the laboratory experiments and the numerical model against the scaling relation. The symbols near the data points correspond to either laboratory (L) or numerical (N) experiments. The dashed line is the best fit $\overline{U}_1/u_0 = (0.9\lambda + 12.7) \times 10^{-2}$.

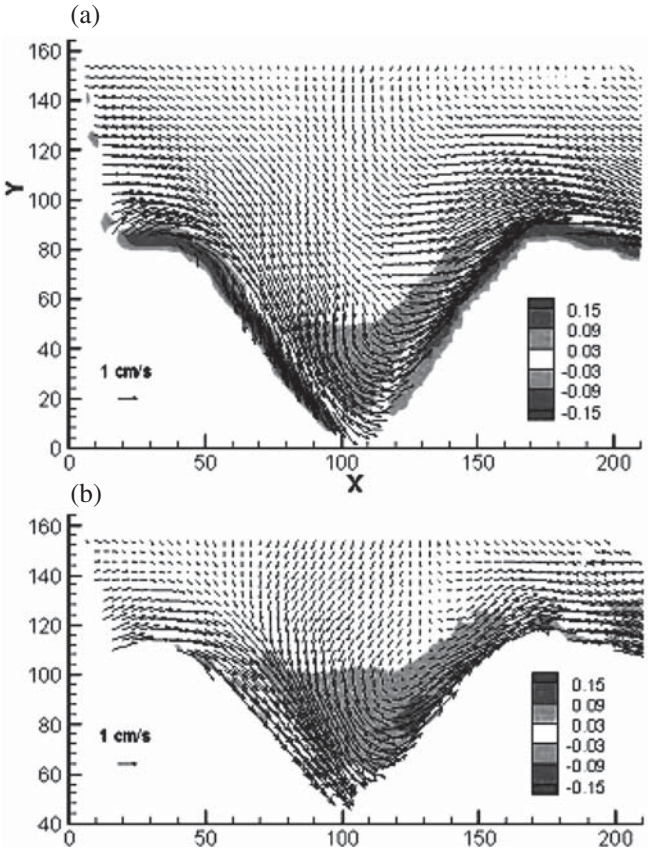

Figure 5. Velocity and vorticity fields for laboratory experiments in Grenoble at the level (a) $z/h_D = -0.2$, (b) $z/h_D = -0.4$. The case without roughness elements. Parameters are given in Table 1.

Figure 4 is a plot of the square root of the mean kinetic energy per unit mass normalized by the amplitude of the forcing current, $\overline{U}_1/u_0$, against the scaling parameter λ defined in (2.3); the data include those obtained from laboratory experiments, labeled L and from numerical experiments, labeled N. We conclude that there is a good support to the scaling arguments advanced.

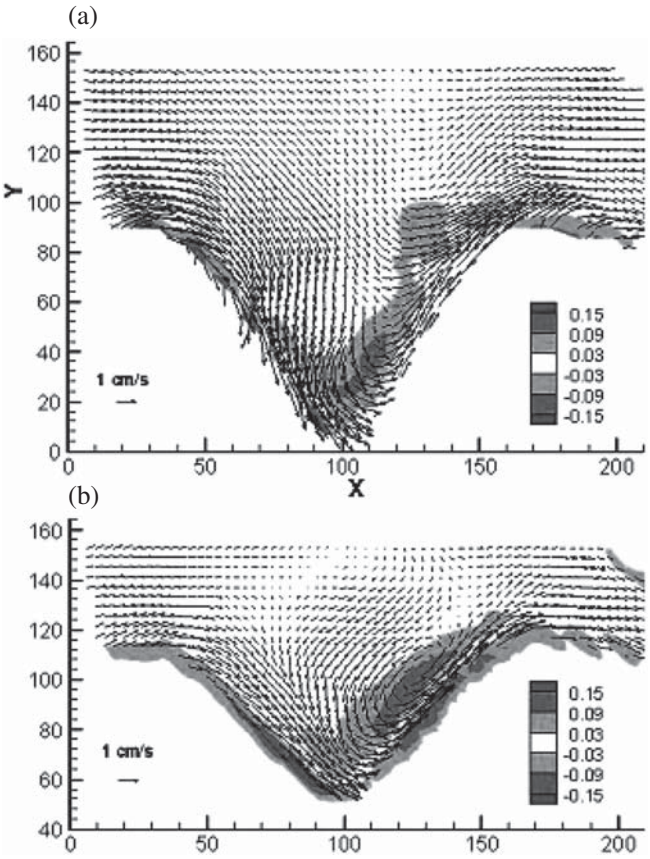

Figure 6. Velocity and vorticity fields for laboratory experiments in Grenoble at the level (a) $z/h_D = -0.2$, (b) $z/h_D = -0.4$. The case with roughness elements. Parameters are given in Table 1.

2.3 *Some experiments with boundary layer turbulence*

Motion fields in the ocean are inherently turbulent and it is thus important to address the question of the modeling of inherently turbulent flows. Figures 5a, b and 6a, b are the plots of the time mean flow and vorticity fields at the shelf break levels $z/h_D = -0.2$ and $z/h_D = -0.4$ of the time mean flow for the case in which the topography is smooth and for the case in which roughness elements of the size 3 cm cubed (separated by a spacing of 15 cm) are placed on the model floor (see Fig. 1b), respectively.

Qualitative comparisons between these Figures and those for the laminar experiments show that the mean flows are qualitatively similar to the turbulent flows. In particular, there is a flow into the canyon from the deep water and flow away from the canyon along its flanks in the upper level. The rectified flows in the upper layers are also predominantly cyclonic and are characterized by jet-like motions along the canyon walls with the coastline on the right facing downstream. As for the laminar flows, there is also a strong time mean flow directed downstream along the continental slope isobaths; i.e., with the coast on the right. Quantitative comparisons of these turbulent flows will be made in a later communication that is now in preparation.

REFERENCES

Boyer, D.L., Haidvogel, D.B. & Pérenne, N. 2003. Laboratory-numerical model comparisons of canyon flows: A parameter study. *J. Phys. Ocean.* Submitted.

Haidvogel, D.B. & Beckman, A. 1998. Numerical modeling of the coastal ocean. In K.H. Brink & A.R. Robinson (eds), The Sea: 457–482. Vol. 10. John Wiley and Sons.

Haidvogel, D.B. & Beckman, A. 1999. Numerical Ocean Circulation Modeling. London: Imperial College Press.

Pedlosky, J. 1979. *Geophysical Fluid Dynamics*. Springer-Verlag.

Perenne, N., Haidvogel, D.B. & Boyer, D.L. 2001. Laboratory-numerical model comparisons of flow over a coastal canyon. *J. Atmos. Oceanic Technol.* 18, 235–255.